



HAL
open science

Larval dispersal simulations and connectivity predictions for Mediterranean gorgonian species: sensitivity to flow representation and biological traits

Roberta Sciascia, Katell Guizien, Marcello Magaldi

► To cite this version:

Roberta Sciascia, Katell Guizien, Marcello Magaldi. Larval dispersal simulations and connectivity predictions for Mediterranean gorgonian species: sensitivity to flow representation and biological traits. ICES Journal of Marine Science, 2022, 10.1093/icesjms/fsac135 . hal-03770887

HAL Id: hal-03770887

<https://hal.science/hal-03770887v1>

Submitted on 6 Sep 2022

HAL is a multi-disciplinary open access archive for the deposit and dissemination of scientific research documents, whether they are published or not. The documents may come from teaching and research institutions in France or abroad, or from public or private research centers.

L'archive ouverte pluridisciplinaire **HAL**, est destinée au dépôt et à la diffusion de documents scientifiques de niveau recherche, publiés ou non, émanant des établissements d'enseignement et de recherche français ou étrangers, des laboratoires publics ou privés.

Larval dispersal simulations and connectivity
predictions for Mediterranean gorgonian species:
sensitivity to flow representation and biological traits.
manuscript for ICES: Journal of Marine Science

Roberta Sciascia

Consiglio Nazionale delle Ricerche (CNR), Istituto di Scienze Marine
(ISMAR), Sede Secondaria di Lerici, Lerici (SP),

19032, Italy

roberta.sciascia@sp.ismar.cnr.it

Katell Guizien

CNRS, Sorbonne Université, Laboratoire d'Ecogéochimie des
Environnements Benthiques, LECOB, Banyuls sur Mer,

F-66650, France

guizien@obs-banyuls.fr

Marcello G. Magaldi

Consiglio Nazionale delle Ricerche (CNR), Istituto di Scienze Marine
(ISMAR), Sede Secondaria di Lerici, Lerici (SP),

19032, Italy

July 4, 2022

Abstract

Larval dispersal enables demographic and genetic connectivity among marine populations. For many sessile species, it is the only natural mechanism for resilience after major population disturbances, as those that have been affecting Mediterranean gorgonian species inside and outside MPAs. Larval dispersal simulation is a powerful tool to anticipate connectivity among populations which might be altered by modelling choices. We assessed how flow representation (resolution and vertical turbulence) and larval traits (pelagic larval duration, release timing and duration, larval vertical behaviour) influenced populations connectivity among five coastal rocky locations in the Northwestern Mediterranean, four of them being designated as MPAs. We used a finer (0.3 km) and coarser (1.5 km) flow resolution in two years to assess, using a hierarchical simulation approach, the sensitivity of connectivity patterns to the above parameters. Larval traits corresponded to two gorgonian species, the neutrally buoyant *Eunicella singularis* and the passive sinker *Paramuricea clavata*. Ocean model resolution was the most influential factor on resulting connectivity patterns. When using the finer flow model resolution, connectivity patterns were equally influenced by all larval traits while vertical turbulence could be neglected. Hence, advising the design of coastal MPAs with regional connectivity estimates requires adequate flow simulation resolution.

Keywords: Larval dispersal modelling; connectivity; larval behaviour; larval traits; NW Mediterranean; *Paramuricea clavata*; *Eunicella singularis*

1 Introduction

1 Anticipating the impact of the on-going global change on the already altered ocean biodi-
2 versity is a major challenge for designing conservation measures for the next decade (ONU

3 SGD 14, IPBES 2030 work program). Among conservation measures, the Aichi Conven-
4 tion on Biological Diversity (CBD, 2010) defined the objective of reaching 10% of ocean
5 surface designated as Marine Protected Areas (MPAs) by 2020. Many studies have shown
6 the efficacy of MPAs on the conservation of fishes and benefits to outside areas through
7 the spillover of juvenile and adult fishes (see Grüss et al., 2011, for a review). MPAs
8 actually conserve habitats in which motile species find food and/or refuge by being geo-
9 graphically confined. An essential component for MPAs attractiveness is the presence of
10 large erected sessile species like corals and gorgonians as they increase habitat complexity
11 and are associated to abundant and diverse vagile species (Ponti et al., 2016). Along the
12 Mediterranean coastline, many gorgonian populations have been reported, outside and
13 inside MPAs. These ecosystem-engineer sessile species are therefore considered as um-
14 brella species and used as indicator of conservation measures efficacy by MPA managers.
15 Yet, the conservation in MPAs of sessile species whose reproduction implies a disper-
16 sive phase mediated by ocean flow poses the question of anticipating population renewal,
17 hence connectivity, within a geographically fragmented network (Halpern and Warner,
18 2003). Extending or modifying the existing network of MPAs requires performing scenar-
19 ios based on sound scientific knowledge (MedPAN, 2017). Designating efficient MPAs
20 requires incorporating knowledge and understanding of mechanisms regulating species
21 spatial distribution, including dispersal (Urban et al., 2016).

22 To this end, larval dispersal numerical models allowing to incorporate knowledge and
23 understanding of mechanisms regulating dispersal are essential tools (Lett et al., 2008;
24 Paris et al., 2013). However, in practice, larval dispersal simulations first require flow sim-
25 ulations to provide a reliable and validated flow representation. Flow variability should
26 be accounted for at spatio-temporal scales relevant for both dispersal processes (larval
27 scale) and regional connectivity estimates (population scale, including demographic vari-
28 ability, North et al., 2009). Connectivity studies have used a variety of ocean circulation
29 models, from coarse-resolution global models (10 km, Wood et al. 2014) to high-resolution
30 regional models (100 m to 1 km, Guizien et al. 2012; Briton et al. 2018). Ocean flow
31 models have been validated against diagnostic variables such as sea surface temperature

32 and salinity, heat content and sea level. However, such validation can be insufficient to
33 ensure that simulated velocities used in the larval dispersal simulations are representa-
34 tive of the advection and diffusion experienced by larvae in the flow (Pineda et al., 2007).
35 When the flow field (speed and direction) simulations are accurate, the specificity of lar-
36 val dispersal simulations ultimately depends on the knowledge of biological traits such
37 as location and timing of larval release in parental populations and larval traits impor-
38 tant for dispersal (Scheltema, 1986). For benthic species, combining underwater imaging
39 techniques with species distribution modelling enables to significantly expand knowledge
40 about parental populations mapping and is now frequently used to parameterize larval
41 dispersal simulations, including those in deeper environments (Metaxas et al., 2019). In
42 contrast, release schedule within the reproductive season is often not known, due to the
43 difficulty of observing such inconspicuous events (except for massive spawners such as
44 corals, Coelho and Lasker, 2014). A recent systematic study of the sources of variance in
45 recruitment patterns along the Chilean coast suggested that nearly half of the variance
46 remained unexplained by PLD, behaviour, release location or season, pointing out to the
47 significance of hydrodynamic stochasticity in coastal wind-driven flows in connectivity
48 patterns (Ospina-Alvarez et al., 2018). Varying the timing of pulse release events within
49 the reproductive season have shown that short term variability in wind-driven flows drives
50 large differences in larval dispersal patterns (Marta-Almeida et al., 2006; Guizien et al.,
51 2012). In presence of short term flow temporal variability, repeating short release events
52 periodically or extending the release duration is essential to increase the persistence of
53 population connections (Guizien et al., 2012; Kough and Paris, 2015; Hock et al., 2019).
54 Once release location and timing are defined, Pelagic Larval Duration (PLD, hereinafter),
55 considered as a primary driver of connectivity, has been extensively tested in larval dis-
56 persal simulations (, reviewed in Swearer et al. 2019). When the PLD was varied, larval
57 dispersal either relied on the neutrally buoyant larvae approximation in three-dimensional
58 simulations (Guizien et al., 2012; Simons et al., 2013) or was restricted to two-dimensional
59 simulations at a fixed depth, often at the surface (Gamoyo et al., 2019). However, larval
60 position in the water column is critical for the dispersal of many benthic species taxa

61 (Corell et al., 2012) and traits regulating the vertical position of benthic species alter
62 their dispersal (Queiroga et al., 2007). Including larval motility behaviour in dispersal
63 modelling requires knowledge on the behaviour of larvae of the species of interest, which
64 implies bridging a gap between modelling and experimentation (Leis, 2021). In summary,
65 the impact of flow field representation choices on connectivity estimates needs to be as-
66 sessed systematically and compared to the effect of varying biological traits (Huret et al.
67 2007).

68 In the present study, we performed a case study for larval dispersal simulations sen-
69 sitivity analysis for two Mediterranean gorgonian species, *Paramuricea clavata* (Risso
70 1826) and *Eunicella singularis* (Esper 1794). We selected five locations in the Ligurian
71 sea where gorgonians have been reported. Four of these locations are designated as MPAs.
72 We addressed first the sensitivity of connectivity predictions among these five locations
73 to flow representation, including horizontal grid resolution and temporal resolution, to-
74 gether with varying basic dispersal parameters such as PLD, release timing and duration.
75 We addressed then the sensitivity to traits regulating larval vertical position, with and
76 without turbulent vertical diffusion. Eventually the sensitivities to the different parame-
77 ters were ranked by importance and commented with respect to connectivity estimates
78 within the current MPA network of the Ligurian Sea.

79 **2 Methods**

80 **2.1 Study background**

81 The Ligurian Sea extends between Italy and the north of Corsica in the Northwestern
82 Mediterranean Sea. It is characterized by a mean cyclonic circulation (Millot, 1999)
83 known as the Ligurian Current (LC) that flows west along the Italian coast toward
84 France (Fig.1). The Ligurian Current is a well studied component of the large scale
85 Mediterranean circulation, however only a very limited number of flow speed observations
86 are available in the summer season along the coastline. We used for validation a time
87 series from an Acoustic Current Doppler Profiler (ADCP) deployed in 2004 in the vicinity

88 of the MT Haven shipwreck (44.37°N, 8.70°E, Fig.1, open triangle).

89 Along the Ligurian coast, many MPAs have been established (Regional Natural Re-
90 serve of Bergeggi, Regional Natural Park of Portofino, Cinque Terre National Park, Re-
91 gional Natural Park of Porto Venere, Fig.1). These MPAs foster the conservation of the
92 rich biodiversity associated to the patchily distributed coralligenous and rocky bottom
93 habitats. In these MPAs, conspicuous gorgonian species such as *Eunicella singularis*
94 and *Paramuricea clavata* have been used as flagship species for the conservation of the
95 Mediterranean coralligenous assemblage (Carpine and Grasshoff, 1975), due to their role
96 of ecosystem engineer (sensu, Jones et al. 1994), and their patrimonial value linked to
97 their beauty.

98 The white gorgonian *Eunicella singularis* is an erected sessile species of about 50 cm
99 height which dwells on rocky bottoms in shallow waters, as well as on coralligenous
100 formations in deeper sublittoral waters (Gori et al., 2011). Each year, *E. singularis*
101 releases lecithotrophic planulae during periods of about 10 days between the end of June
102 and early July (Ribes et al., 2007). *E. singularis* larvae swim during 45 to 91% of the
103 time, compensating for their negative buoyancy. In a laboratory experiment, these larvae
104 maintained themselves at 20°C in the middle of the sea water container, just like neutrally
105 buoyant larvae (Guizien et al., 2020).

106 The red gorgonian *Paramuricea clavata* is one of the tallest sessile Mediterranean
107 species with erected colonies as high as 1.3 m and is found on hard substrate from 10
108 to 200 m water depth (Gori et al., 2017). During reproduction, *P. clavata* releases eggs
109 that get fecundated and mature within a few days at the colony surface. Once the
110 maternal mucus is dissolved, lecithotrophic planula larvae are released in the ocean flow.
111 *P. clavata* larvae are non-motile and sink in sea water at 20°C (Guizien et al., 2020). Off
112 the Catalan coast, larval release happens during short events of a few days separated by
113 15 days (Coma et al., 1995; Gori et al., 2007) in late June/early July. No information
114 on the exact timing and occurrence of *P. clavata* larval release in the Ligurian Sea are
115 available in the scientific literature but several observations by recreational divers report
116 a similar phenomenon in the month of July. For the two species, the competency period

117 extends from a few days to more than 30 days (Guizien et al., 2020; Zelli et al., 2020).

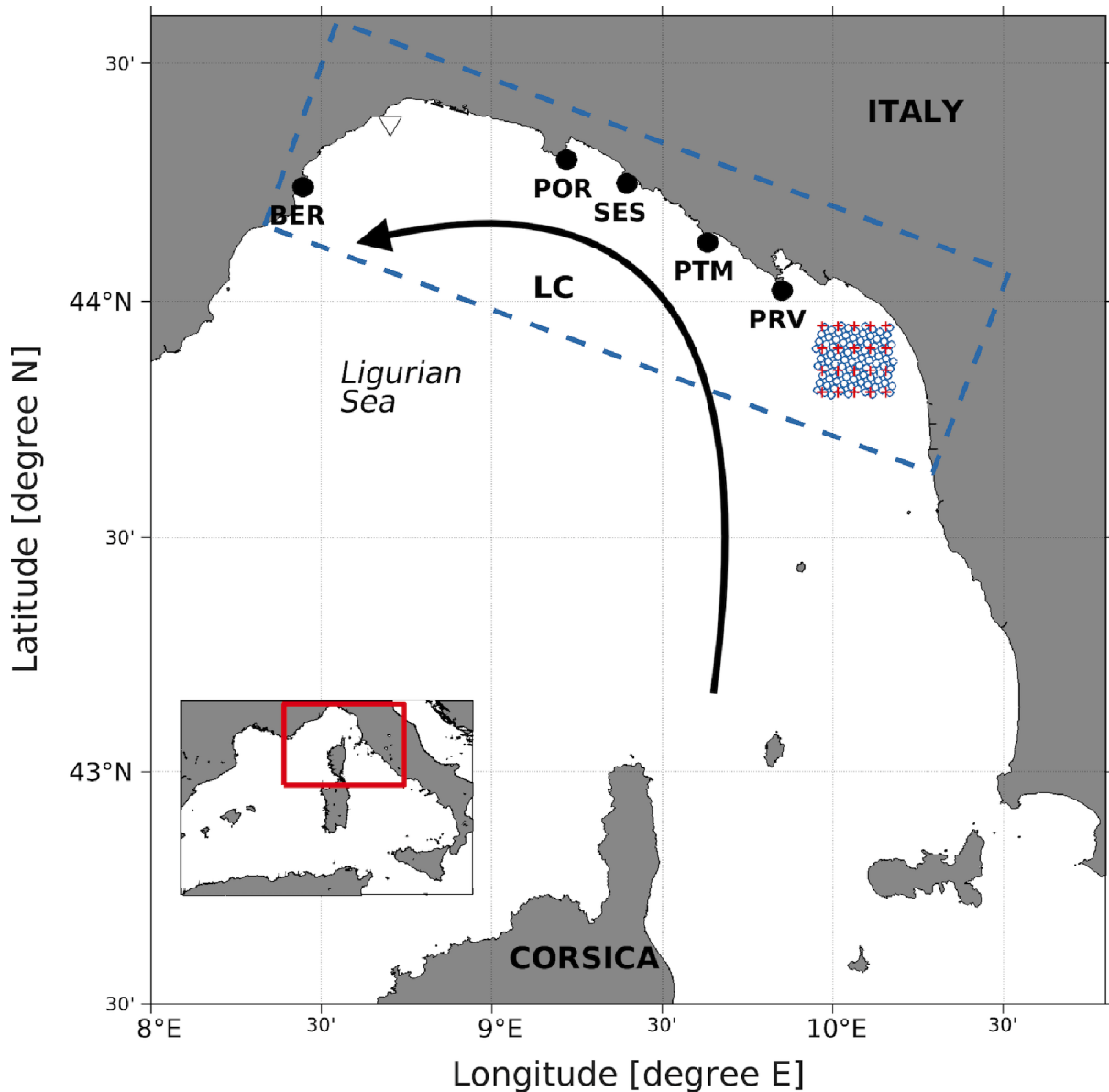


Figure 1: The Ligurian Sea. The arrow depicts the main circulation branch and black circles indicate the release locations used in larval dispersal simulations (see Tab. S1 in the Supp. Inf. for the precise locations). The open triangle indicates the location of the Acoustic Doppler Current Profiler used for flow data validation. Blue dashed rectangle shows the LIMEgcm (fine resolution) domain while the red rectangle in the inset shows the LIME-ROMS (coarse resolution) domain. Blue circles display every 6 grid points of the the LIMEgcm mesh and red crosses display every 3 grid points of the LIME-ROMS mesh.

118 **2.2 3D flow simulations at coarse and fine resolutions**

119 The circulation of the Ligurian Sea was simulated at two grid resolutions in 2004 and
120 2006, with the aim of describing the inter-annual variability in the stratified summer
121 circulation while limiting the number of simulations. In fact, the largest deviation in the
122 Mediterranean summer sea surface temperature over the 2003 – 2019 period was observed
123 between 2004 and 2006 (García-Monteiro et al., 2022) and an abrupt shift in the Western
124 Mediterranean circulation was observed starting from 2005 (Schroeder et al., 2016).

125 The coarser resolution 3D flow simulations hereinafter called Ligurian Integrated
126 Modelling Effort-ROMS (LIME-ROMS, Sciascia et al. 2019) was based on the Rutgers
127 University kernel of the Regional Ocean Modelling System (ROMS, Shchepetkin and
128 McWilliams 2005). The numerical domain was discretized with an horizontal grid of 590
129 x 314 points. The mesh was unevenly spaced and the most resolved area (Fig.1, red
130 rectangle), which includes the area of the Ligurian-Northern Tyrrhenian shelf, had a hor-
131 izontal resolution of $1/64^\circ \times 1/64^\circ$ (~ 1.5 km, Fig.1, red crosses). The vertical dimension
132 was discretized with 50 sigma layers. Realistic surface forcings came from the 3-hourly,
133 0.25° horizontal resolution ERA-Interim reanalysis fields (Dee et al., 2011), while the daily
134 open boundary values were derived from the Mediterranean Forecasting System (MFS)
135 SYS4a3 product. Model outputs were saved every six hours. The reader is referred to
136 Sciascia et al. (2019) for a detailed description and evaluation of the hydrodynamical
137 model performance.

138 The fine resolution 3D flow simulations hereinafter called Ligurian Integrated Mod-
139 elling Effort gcm (LIMEgcm, Fig.1 blue dashed rectangle) was based on the Massachusetts
140 Institute of Technology general circulation model (MITgcm, Marshall et al. 1997). The
141 MITgcm solves the Boussinesq form of the Navier–Stokes equations either on a genera-
142 lized curvilinear grid or an orthogonal grid. The finite-volume discretization is rendered
143 on a horizontal Arakawa C-grid with vertical z levels. In this configuration the equation
144 of state is due to Jackett and McDougall (1995) and the advection of tracers is computed
145 via a third-order direct space–time flux limited scheme with zero explicit diffusivity. The
146 K-profile parameterization (KPP, Large et al. 1994) is used with a background vertical

147 viscosity of $10^{-5} \text{ m}^2\text{s}^{-1}$. The numerical domain was discretized with an orthogonal hor-
148 izontal grid of 560×160 points. The horizontal mesh had a resolution of 300 m (Fig.1,
149 blue circles) while the vertical was discretized with 100 levels. The vertical resolution
150 increased linearly from 1 m to 20 m in the first 20 levels, was kept constant at 20 m
151 for the following 50 levels, and finally increased to 25 m for the 30 deepest layers. The
152 bathymetry is interpolated from the EMODNET 1/8 arcminute product. Realistic sur-
153 face forcings came from the hourly, Weather Research and Forecasting (WRF) model
154 setup by the University of Genoa (Cassola et al., 2015), while 6-hourly open boundary
155 conditions were derived from LIME-ROMS model outputs (Sciascia et al., 2019). Model
156 outputs were saved every three hours.

157 **2.3 Larval dispersal simulations**

158 Dispersal simulations of virtual larvae were performed independently using the LIME-
159 ROMS (hereinafter, coarse) and LIMEgcm (hereinafter, fine) simulations.

160 The offline Lagrangian Transport model (LTRANS, Schlag and North 2012) was se-
161 lected to compute particle advection in the coarse resolution flow field for its capability
162 to cope with sigma layers. The offline Connectivity Modelling System (CMS, Paris et al.
163 2013) was selected to compute particle advection in the fine resolution flow field for its
164 capability to cope with z layers. Both Lagrangian models compute 3D trajectories us-
165 ing a 4th-order Runge-Kutta scheme and can describe neutrally buoyant and active (e.g.
166 sinking, swimming) particles, eventually including horizontal and/or vertical turbulent
167 diffusion to represent horizontal and/or vertical motions at scales smaller than the grid
168 resolution of the flow models.

169 In the present study, particles were released in five locations Bergeggi (BER), Portofino
170 (POR), Sestri Levante (SES), Punta Mesco (PTM), and Porto Venere (PRV), all being
171 MPAs except SES (Fig. 1, Supp. Inf. Tab. S1). Each location was described by ten
172 release points, separated by 100 m. Particles were released ~ 3 km away from the coast
173 line and 4 m above the bottom in the coarse resolution simulations and 2 m above the
174 bottom in the fine resolution simulations in order to avoid any retention bias due to the

175 bottom numerical boundary layer (Supp. Inf., Tab. S1). In all larval dispersal simulation
176 setups, particles were tracked with a tracking time step of 600 s, ensuring that no particle
177 crossed a grid cell within one timestep at the fastest flow speed.

178 The hierarchical simulation design used in this study consisted of eight larval dispersal
179 simulation experiments (Tab. 1). In a first group of experiments, the effect of the flow
180 field representation (in space and time) was quantified for neutrally buoyant particles
181 by comparing purely Lagrangian simulations using both the coarse and fine resolution
182 flow representation, the latter varying the flow update frequency between 6h and 3h
183 (Exp. 1, 2 and 3 in Tab. 1). In a second set of experiments, the effect of the different
184 larval vertical behaviour of two gorgonian species and vertical turbulence were quantified
185 applying a fully factorial set up (from Exp. 3 to 8 in Tab. 1). In this case, only the fine
186 resolution flow representation was considered as it was shown to best agree with current
187 speed observations in the area and Exp.3 was considered as reference simulation (see
188 Results section). In all larval dispersal simulation experiments (from Exp. 1 to 8, Tab.
189 1), particles were released every hour from June 15 at midnight until July 15 at 11 pm
190 for both 2004 and 2006 and tracked for 28 days, according to their competency ability
191 (Zelli et al., 2020).

192 The neutrally buoyant particles would actually represent the motile *E. singularis*
193 larvae, which swimming behaviour compensates their negative buoyancy (Padrón et al.,
194 2018a). The non-motile *P. clavata* larvae (Coma et al., 1995; Linares et al., 2008) were
195 represented as particles with a negative buoyancy. For *P. clavata*, particle density was
196 set to vary between 1.0282 and 1.0295 (a value within this range is randomly sorted at
197 each time step), with an equivalent diameter of 761 μm , to achieve the sinking speed
198 of $0.056 \pm 0.021 \text{ cm s}^{-1}$ at 20°C and a salinity of 38 psu as measured experimentally
199 (Guizien et al., 2020). Hence, *P. clavata* larvae behaviour would change according to the
200 surrounding sea water density. For example in summer, they would sink in the upper and
201 lighter part of the ocean but float when dispersed in the deeper and denser ocean layers.

202 Three levels of vertical subgrid turbulence intensity were tested by repeating each
203 simulation without turbulence, and with a constant low (Munk, 1966, i.e. $10^{-4} \text{ m}^2 \text{ s}^{-1}$) or

Experiment	Flow horizontal resolution	Flow update frequency	Larval vertical behaviour	Turbulence
Exp.1	Coarse	6 hours	<i>E. singularis</i>	No
Exp.2	Fine	6 hours	<i>E. singularis</i>	No
Exp.3	Fine	3 hours	<i>E. singularis</i>	No
Exp.4	Fine	3 hours	<i>E. singularis</i>	Low ($10^{-4} \text{ m}^2\text{s}^{-1}$)
Exp.5	Fine	3 hours	<i>E. singularis</i>	High ($10^{-3} \text{ m}^2\text{s}^{-1}$)
Exp.6	Fine	3 hours	<i>P. clavata</i>	No
Exp.7	Fine	3 hours	<i>P. clavata</i>	Low ($10^{-4} \text{ m}^2\text{s}^{-1}$)
Exp.8	Fine	3 hours	<i>P. clavata</i>	High ($10^{-3} \text{ m}^2\text{s}^{-1}$)

Table 1: Larval dispersal simulations setup. Particles were released every hour from June 15 at midnight until July 15 at 11pm for both 2004 and 2006 and tracked for 28 days after release. The total number of particles released each year is 36000 (1 release per hour) for Exp.1, 2 and 3 and 900000 (25 release per hour) for Exp.4, 5, 6, 7 and 8. The reference simulation is indicated in bold.

204 high ($10^{-3} \text{ m}^2 \text{ s}^{-1}$) turbulent diffusivity (Tab. 1). Depending on whether larval behaviour
205 and/or turbulence was (was not) accounted for, twenty-five (one) particles were released
206 every hour during the entire reproductive period to reach a sufficient number of released
207 particles ensuring the convergence of connectivity matrices (Guizien et al., 2006; Simons
208 et al., 2013).

209 2.4 Connectivity predictions

210 Larval transport values between the five locations in the Ligurian sea were calculated as
211 the proportion of particles released during a release event from an origin location that
212 reached a destination location after a given PLD. Release events were defined by their
213 timing and duration. The duration of a release event was varied between 3, 9 and 30 days,
214 the latter representing the entire reproductive period. For each release event duration,
215 a set of non-overlapping release events were built spanning the 30-day long reproductive
216 season of each year (2004 and 2006), yielding twenty 3-day, six 10-day and two 30-day
217 release events. In total, for each of the eight larval dispersal simulation experiments
218 (Tab.1), 252 connectivity predictions were built, varying the PLD (9 levels: 1, 3.5, 7,
219 10.5, 14, 17.5, 21, 24.5 and 28 days) and the release event duration and timing (3 levels:
220 3, 9 and 30 days, with 20, 6 and 2 replicates, respectively).

221 The following metrics were defined to quantify the effect of the release timing vari-
 222 ability for each PLD:

$$\sigma_{intra} = \sqrt{\frac{\sum_{y=1}^{N_y} \sum_{r=1}^{N_r} (T_r^y - \overline{T^y})^2}{N_r N_y}} \quad (1)$$

223

$$\sigma_{inter} = \sqrt{\frac{\sum_{r=1}^{N_r} \sum_{y=1}^{N_y} (T_r^y - \overline{T_r})^2}{N_r N_y}} \quad (2)$$

224 where N_y is the number of years, N_r is the number of release events per year and $\overline{T^y} =$
 225 $\sum_{r=1}^{N_r} T_r^y / N_r$ is the average connectivity across all release events of year y and $\overline{T_r} = \sum_{y=1}^{N_y} T_r^y / N_y$
 226 is the average connectivity across all years for the release event r in the year. Those
 227 metrics decomposed the release timing variability into a within-year (σ_{intra} , standard
 228 deviation around the annual mean) and a between-year (σ_{inter} , standard deviation around
 229 the release timing mean among years) contribution. Note that in equations (1) and
 230 (2), T stands for any element T_{ij} of the connectivity matrix between a release i and
 231 destination j location, and a given PLD value. Those metrics were estimated for each
 232 pairwise connection among the five locations network. Boxplots were used to display the
 233 statistical distribution of σ_{inter} and σ_{intra} in the connectivity matrices for each PLD and
 234 release duration in Exp. 1 and 3.

235 To compare the effects of the flow simulation horizontal resolution and update fre-
 236 quency, of the larval vertical behaviour and of the turbulence level on connectivity pre-
 237 dictions within the five-location network, deviations between any experiment and the
 238 reference experiment Exp.3 were calculated for each larval transport connection, for a
 239 same PLD and release event. The deviations in the different release events were described
 240 by their median to avoid any normality assumption. All calculations and statistics were
 241 conducted in Matlab (R2018).

242 **3 Results**

243 Exp.1, 2 and 3 were designed to test the usual practice of increasing both spatial reso-
244 lution and update frequency when considering finer resolution models. In both fine and
245 coarse flow resolution (Exp.1 vs Exp.3), the median connectivity matrix among the five
246 populations displayed a northwestern drift (upper diagonal elements larger than lower
247 diagonal ones), with larval export (off-diagonal elements) from PRV and SES dominating
248 over local retention (diagonal elements) and retention rates dominated over any other
249 connections in BER, POR and PTM for a PLD of 3.5 days (Fig. 2). For the same PLD,
250 varying the update frequency of the fine resolution flow field representation from three
251 to six hours, i.e. same of the coarse resolution simulations (Exp.2 vs Exp.3), did not
252 alter the median connectivity matrix (Fig. S1 in the Supp. Inf.). The sensitivity to
253 update frequency in the fine resolution experiments was negligible across all PLDs (data
254 not shown).

255 Extending the comparison of Exp.1 and Exp.3 to all PLDs showed that the sets of
256 simulations with different spatial resolution differed largely (Supp. Inf. Fig. S2). Firstly,
257 for short PLDs, larval retention values were ten times larger using the coarse resolution
258 flow representation (max $\sim 95\%$) compared to the fine resolution one (max $\sim 7\%$) with
259 largest retention values found in different locations (BER and POR in the coarse reso-
260 lution and PTM in the fine resolution; Fig. 2 a,b). Secondly, more connections between
261 populations appeared when the PLD increased using the finer resolution of the flow re-
262 presentation. Finally, connectivity predictions varied little when PLD was varied from
263 1 to 28 days using the coarser resolution. In contrast, larval transport values decreased
264 drastically when PLD decreased from 1 to 10.5 days and became negligible across the
265 network of the five populations for PLD larger than 14 days using the finer resolution.

266 Differences in the intensity of coastal currents when varying the resolution of the flow
267 representation explain the differences in larval transport estimates. Coastal currents were
268 weaker in the coarse resolution flow representation compared to the fine resolution one
269 (Figs. S3 and S4 in the Supp. Inf.). For the period May-June 2004, despite the temporal
270 mismatch of the high speed events occurrence, statistically, observed flow speed quantiles

	10%	25%	50%	60%	70%	80%	90%
Observations	3.2	5.9	10.8	13.5	16.6	20.6	26.0
Fine resolution (Exp.3)	4.1	6.8	12.0	14.0	16.2	19.0	24.0
Coarse resolution (Exp.1)	3.2	6.1	9.3	10.5	12.0	14.0	17.6

Table 2: Quantiles of flow speed in cm s^{-1} at the location of the ADCP over a two-month summer period (15/05/2004-15/07/2004) for the observations, and the fine and coarse resolution simulations.

271 corresponding to these events were better predicted in the fine resolution simulation than
 272 in the coarse one (Tab. 2).

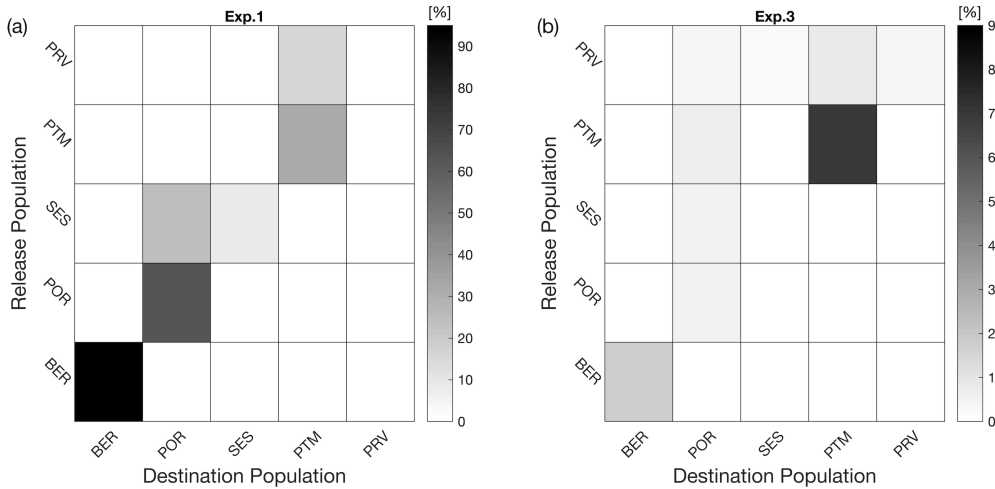


Figure 2: Median connectivity matrix for a PLD of 3.5 days and a 3-day release duration in (a) Exp.1 with coarse resolution flow representation updated every 6h and in (b) Exp.3 with fine resolution flow representation updated every 3h.

273 We then explored the effect on connectivity predictions of the interaction between
 274 the flow dynamics simulated at coarse and fine resolution and the larval release timing.
 275 Connectivity matrices showed temporal variability at both resolutions. This temporal
 276 variability was described by two contributions, the between-year and within-year standard
 277 deviation (σ_{intra} and σ_{inter} , Fig. 3 and Fig. S5 of the Supp. Inf.). When larval release
 278 timing extended over the entire 30-day reproductive period, the temporal variability
 279 equals the between-year variability and was minimum, whatever the flow resolution (Fig.
 280 3a and b). Temporal variability increased both between-year and within-year when the
 281 release duration decreased, for all PLDs and whatever the flow resolution. Moreover,
 282 within-year variability (σ_{intra}) and between-year variability (σ_{inter}) were the same order
 283 of magnitude. The within-year to between-year standard deviation ratio was around 1.2

284 for both resolutions, whatever the release duration and across all PLDs. This indicates
 285 that the temporal variability of connectivity predictions can be assessed varying the
 286 release timing within a single simulation year. The importance of temporal variability was
 287 different in the coarse and fine resolution simulations. In the coarse resolution simulations,
 288 the larval transport standard deviation varied little with PLD and reached at maximum
 289 26%, which is a third of the median larval transport. In the fine resolution simulations,
 290 the larval transport standard deviation decreased with PLD, and reached up to 100% of
 291 the median transfer rates (Fig. S5b vs Fig. 2)).

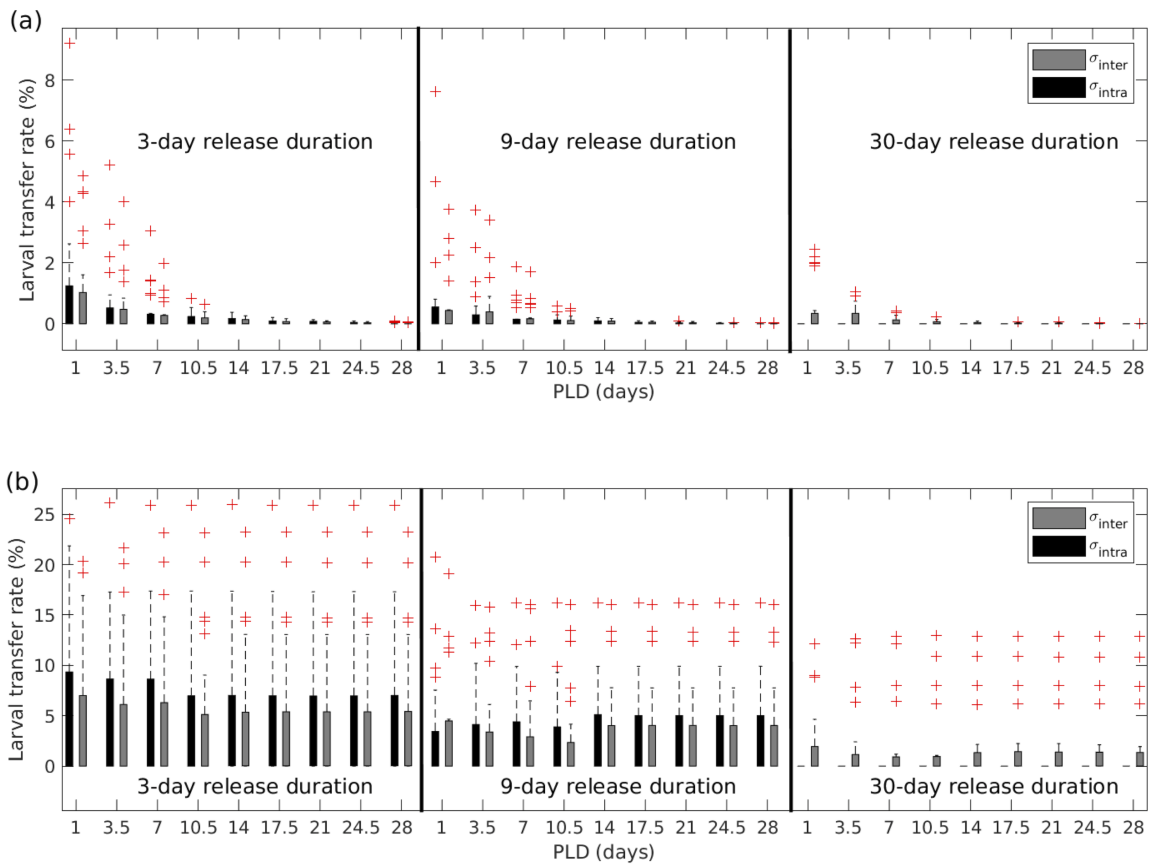


Figure 3: Boxplots of the σ_{intra} (black bars) and σ_{inter} (grey bars) distributions for different PLDs and for different release duration for the Exp.3 (a) and Exp.1 (b) simulations.

292 The sensitivity of connectivity predictions to other parameters was explored next
 293 using the fine resolution flow and quantitatively compared to the sensitivity to horizontal
 294 resolution (Fig. 4a and Fig. 5a). Those parameters were the species specific larval vertical
 295 behaviour of *E. singularis* and *P. clavata* (Fig.4b and 5b) and different vertical turbulence
 296 levels (Fig.4 c,d and 5c,d). A clear hierarchy can be drawn with the effect of the flow

297 representation resolution being an order of magnitude higher (median deviation up to
 298 90%) than that of incorporating the specific behaviour (median deviation up to 14%) and
 299 two orders of magnitude higher than the effect of including turbulence dispersal, whatever
 300 the level (median deviation up to 5% for the two levels of turbulence tested, Fig.4c,d).
 301 More specifically, the effect of incorporating the specific behaviour of *E. singularis* and
 302 *P. clavata* mainly affected the retention rates in PTM, PRV and to a lower extent in
 303 SES (Fig.4 b). The effect on all other connections was similarly negligible. The effect of
 304 turbulence dispersal only affected retention in PTM (Fig.4 c,d).

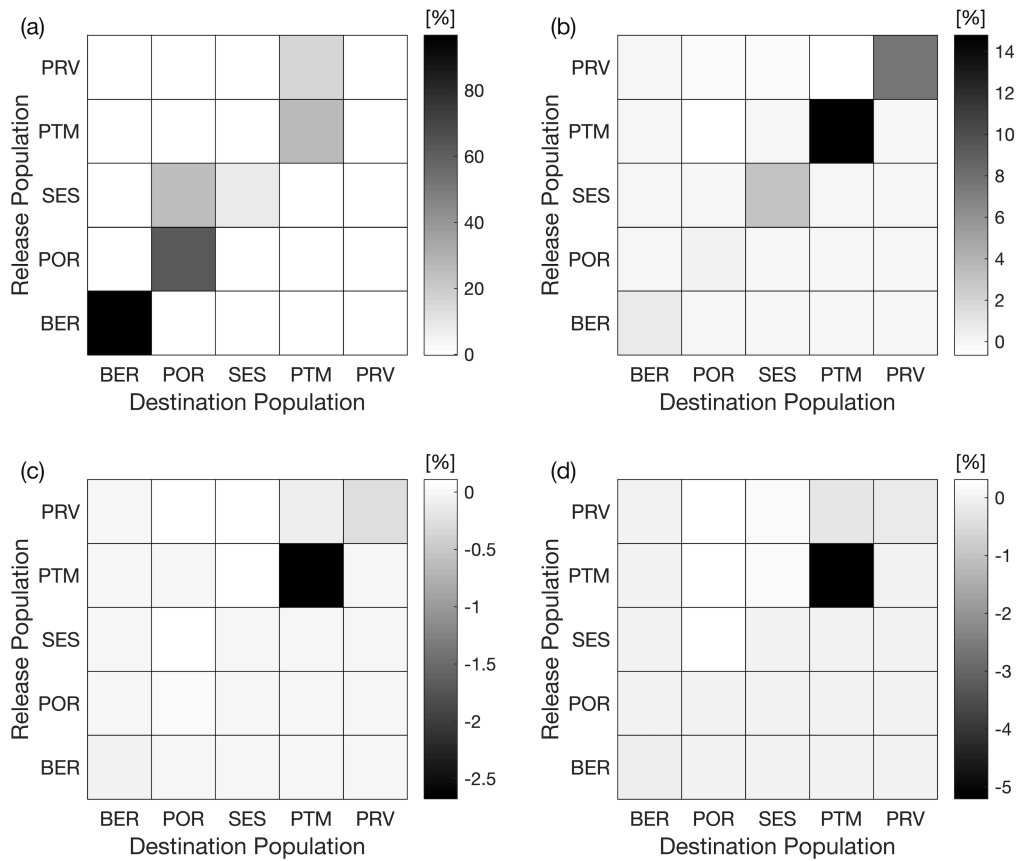


Figure 4: Median of deviation between connectivity matrices in different experiments to the same reference Exp.3 for a PLD of 3.5 days. The different panels display the sensitivity to the resolution of the flow representation (Exp.1 - Exp.3, a), to larval vertical behaviour (Exp.6 - Exp.3, b), to a low vertical turbulence (Exp.4 - Exp.3, c) and a high vertical turbulence (Exp.5 - Exp.3, d).

305 In particular, larval vertical behaviour affected similarly the spatial structure of con-
 306 nectivity for all simulations with short PLDs and turbulence was always negligible (1-7

307 days, data not shown). For longer PLDs (10.5-28 days), sensitivity to the specific buoy-
 308 ancy of *E. singularis* and *P. clavata* and to turbulence intensity were significantly reduced,
 309 although specific behaviour effect remained prevalent (Fig.5 for a PLD of 28 days). While
 310 the specific behaviour continued to affect mainly retention rates when the PLD increase
 311 from 3.5 to 28 days (although in different locations, Fig.4b and Fig.5b), the effect of
 312 turbulence mainly affected distant connections (import for BER, Fig.5c and d).

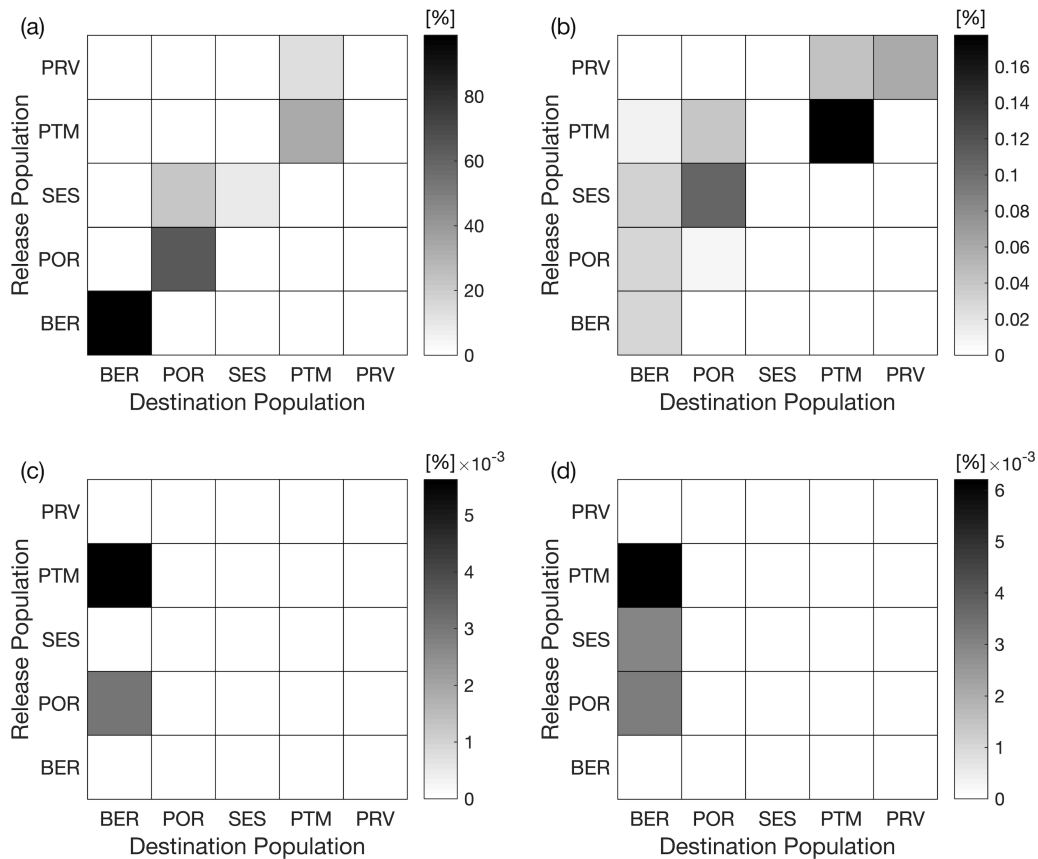


Figure 5: Same as 4 but for a PLD of 28 days

313 Finally, the sensitivity to larval behaviour and turbulence was compared to the sen-
 314 sitivity to PLD. We selected lower range PLD values (1-7 days) as those are the ones
 315 affecting connectivity patterns the most (Fig.S2 in the Supp. Inf.). Varying the PLD
 316 from 3.5 to 1 or 7 days affected larval transport estimates of the same order of magnitude
 317 as those obtained by incorporating *P. clavata* larval vertical behaviour for the PLD of
 318 3.5 days (Fig.6). Reducing the PLD from 3.5 days to 1 day only increased the retention
 319 rates (Fig. 6a) while extending the PLD from 3.5 to 7 days not only decreased retention

320 rates but also distant connections from SES to POR and from PRV to PTM (Fig. 6b).

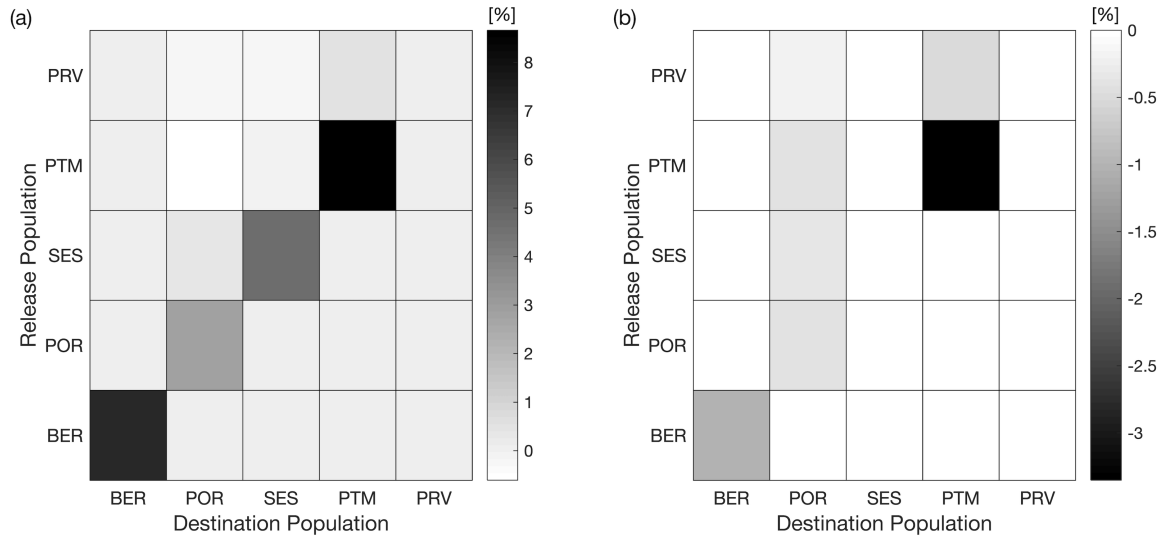


Figure 6: Median of deviation between connectivity matrices in the same reference Exp.3 between (a) a PLD of 1 day, (b) a PLD of 7 days and a PLD of 3.5 days.

321 4 Discussion

322 In the present study we tested the sensitivity of connectivity predictions among gorgonian
 323 populations dwelling in the Ligurian Sea MPAs to parameters used in larval transport
 324 simulations. The horizontal spatial resolution of the hydrodynamical models was found
 325 to have the strongest effect on larval transport. Using the finest resolution flow repre-
 326 sentation, larval behaviour of different gorgonian species and PLD had similar effects on
 327 connectivity predictions, while vertical turbulent diffusion was found to have a second
 328 order effect. Thanks to the progresses in ocean modelling availability and performances,
 329 larval transport predictions are now frequently used to explore the functioning of ma-
 330 rine populations and help understanding their spatial distribution (reviewed in Swearer
 331 et al. 2019). Assessing the accuracy of larval transport predictions is more than often
 332 qualitative (Barbut et al., 2019; Crosbie et al., 2019). However, quantifying the sensi-
 333 tivity of larval transport simulations to the improvements in flow modelling (i.e. flow
 334 representation) and larval traits knowledge (i.e. PLD, larval behaviour, release events)
 335 is preliminary to assess the accuracy of larval transport predictions and connectivity

336 patterns used to identify MPAs networks.

337 The importance of hydrodynamical ocean model spatial resolution in affecting the di-
338 persal patterns of larval transport simulations has been raised in several studies (Guizien
339 et al., 2006; Huret et al., 2007; Putman and He, 2013) and reviewed in Swearer et al.
340 (2019). After comparing two ocean model resolutions of 4 km and 1.6 km, with and
341 without larval vertical behaviour in different years, a recent sensitivity study reported
342 that inter-annual variability was the most influential factor in dispersal simulations of fish
343 larvae in the North Sea (Kvile et al., 2018). The present study showed in contrast that
344 the most influential factor for gorgonian coastal populations in the Ligurian Sea was the
345 flow model resolution as retention increased dramatically when increasing the horizontal
346 cell size from 300 m km to 1.5 km, over-passing the variability of the circulation in two
347 highly contrasting years.

348 Such bias is to be expected in large scale ocean models when the habitat lies within
349 the coastal boundary layer where the model representation of the flow is inaccurate due
350 to both their coarse resolution and their lack of coastal ocean process parameterization
351 (Griffies and Treguier, 2013). For instance, the internal Rossby radius and the geomor-
352 phological features in the North Western Mediterranean coastal zone have dimensions of
353 the same order of magnitude as the coarse resolution used in the present study (Beuvier
354 et al., 2012). The large deviation in connectivity fluxes found in the present study when
355 increasing ocean model resolution advocates to take with caution past studies using basin
356 or Ocean General Circulation ocean Models (OGCM) to evaluate coastal MPAs connec-
357 tivity (Corell et al., 2012; Andrello et al., 2013). In the present study, despite the coarser
358 resolution of 1.5 km was already four times finer than the one used in these past studies
359 (6-7 km), connectivity among the four Ligurian MPAs varied notably when the resolu-
360 tion was further increased. Specifically, the relative status of the four MPAs changed
361 with Bergeggi and Portofino being the most retentive in the coarse resolution predictions
362 while Punta Mesco became the most retentive in the fine resolution predictions. Another
363 difference was the separation of the four MPAs into three clusters in the coarse reso-
364 lution predictions while the fine resolution predictions indicate that the three MPAs of

365 Portofino, Punta Mesco and Porto Venere are connected, Bergeggi being the only isolated
366 MPA. The present study exemplifies the importance of basic methodological choices such
367 as the driving flow representation when science is used to inform management.

368 Large-scale models have an interest to delineate well-connected oceanic regions, when
369 care is taken of releasing particles outside this artefactual coastal numerical boundary
370 layer (Rossi et al., 2014). Delineating such well-connected regions is essential to identify
371 areas in which ocean circulation downscaled simulations should be performed to study
372 specific populations connectivity. To this respect, including turbulence into dispersal
373 simulations is expected to be less important when the cell size decrease as mesoscale and
374 sub-mesoscale processes will be resolved (Guizien et al., 2006; Huret et al., 2007). In
375 the present study, the effect of vertical turbulent diffusion on connectivity patterns was
376 indeed negligible when resolving the coastal circulation at 300 m compared to the effect
377 of biological traits.

378 Among biological traits used in larval dispersal simulations, PLD is a basic one as it
379 defines the tracking duration. Several recent works still performed 2D or 3D dispersal
380 varying PLD only (Gamoyo et al., 2019; Hidalgo et al., 2019). In the present study, con-
381 nectivity predictions varied largely when the PLD varied from 1 to 7 days, but sensitivity
382 to PLD decreased when PLD increased beyond 10 days. Larvae of the few tropical and
383 temperate gorgonian species, whose larval traits have been studied, reached competency
384 after a few days but could survive few weeks in laboratory experiments (Fine et al., 2005;
385 Coelho and Lasker, 2016; Guizien et al., 2020; Zelli et al., 2020). As a result, PLD is
386 a very uncertain parameter in coral species as extended competency seems common for
387 their lecithotrophic larvae thanks to metabolic rate reduction (Graham et al., 2013). In the
388 few larval dispersal modelling studies that targeted gorgonian species, PLDs were varied
389 from a few days to several weeks (Padrón et al., 2018a; Kenchington et al., 2019; Liu et al.,
390 2021). However, despite PLD could extend up to two months, environmental mortality
391 processes occurring during dispersal, such as predation which is removed in the laboratory
392 (Rumrill, 1990), most likely reduce actual PLD in the field. For instance, for the white
393 gorgonian *E. singularis*, the most likely effective PLD determined by comparing dispersal

394 patterns simulations with population genetics in the Gulf of Lion (Padrón et al., 2018a)
395 lied in the lower range of potential PLDs determined experimentally (Guizien et al., 2020).
396 Similarly, for the red gorgonian *P. clavata*, population genetics indicated short distance
397 dispersal to be the most frequent. Yet, observation of long distance migrants suggests
398 that the larger potential PLD observed in laboratory experiments may also contribute
399 to population genetics (Mokhtar-Jamaï et al., 2011; Guizien et al., 2020). In summary,
400 larval dispersal studies for gorgonian species should systematically assess the sensitivity
401 to PLD over a wide competency window.

402 It has been recurrently argued that including larval motility behaviour was key to
403 improve the realism of larval dispersal predictions, and led to develop tracking softwares
404 specific for larval dispersal studies (Lett et al., 2008; North et al., 2009; Schlag and North,
405 2012; Paris et al., 2013). This is considered particularly relevant for the dispersal of fish
406 larvae that can orient themselves and whose swimming speeds are the same order of
407 magnitude as the horizontal flow speed (Leis, 2007, 2021). In contrast, most benthic
408 invertebrates produce larvae unable to outcompete horizontal flow speeds which means
409 passive dispersal in the horizontal (Chia et al., 1984). Yet, larval buoyancy combined to
410 vertical swimming behaviour regulate benthic invertebrate larvae position in the water
411 column, which was shown to alter their dispersal (Guizien et al., 2006; Marta-Almeida
412 et al., 2006; Corell et al., 2012). However, including behaviour in larval dispersal stud-
413 ies of benthic invertebrates remains limited to species with largest vertical swimming
414 speeds such as the diel vertical migration of crustacean species (Queiroga et al., 2007),
415 and oysters (North et al., 2008) or scallops (Tremblay et al., 1994). When larval vertical
416 behaviour was assumed negligible, two dispersal procedures, either two-dimensional at
417 fixed depth or three-dimensional driven by flow vertical velocities have been used. These
418 have been indifferently termed “passive” (Gamoyo et al., 2019; Kenchington et al., 2019;
419 Metaxas et al., 2019). Actually, none of these dispersal simulation approaches should be
420 termed “passive”, as both implicitly assume a larval vertical behaviour with continuous
421 adjustment of larval buoyancy to varying surrounding sea water density. The present
422 study exemplifies that moderate differences in larval vertical behaviour in two gorgonian

423 species, one passive drifter represented by negative buoyancy and the other active swim-
424 mer represented by neutral buoyancy, varied retention in the populations of Porto Venere,
425 Punta Mesco and Sestri Levante. This result suggests to re-cast previous estimates based
426 on two-dimensional dispersal at a prescribed depth for those same species (Rossi et al.,
427 2020). Recent knowledge advances about larval vertical behaviour within the subset of
428 gorgonian species should encourage us to re-cast connectivity predictions including be-
429 haviours explicitly in dispersal simulations (Coelho and Lasker, 2016; Guizien et al.,
430 2020).

431 Release duration is another reproductive trait that was shown to affect the stabi-
432 lity of connectivity patterns (Guizien et al., 2012; Hock et al., 2019). Release duration
433 varies largely among gorgonian species from synchronized short pulses in spawning species
434 (Coma et al., 1995; Coelho and Lasker, 2016) to continuous release in brooding species
435 (Coelho and Lasker, 2014). In the two gorgonian species considered in the present study
436 larval release happens in a few short pulses which timing varies between years during the
437 reproductive season and seems unpredictable (Coma et al., 1995; Ribes et al., 2007). The
438 present study showed that such traits result in uncertain connectivity predictions, which
439 variability can be equally estimated using within- or between-year statistics. A similar
440 increase in connectivity predictions variability when release duration decreased was al-
441 ready reported in the Gulf of Lion, a region displaying similar short-term atmospherical
442 variability to the Ligurian Sea (Vignudelli et al., 1999; Briton et al., 2018). Moreover,
443 for the two gorgonian species in the Ligurian Sea considered in this study, sensitivity to
444 release timing could reach up to 100% of median larval transport values and was the same
445 order of magnitude as to sinking behaviour. As a consequence, connectivity predictions
446 in these two gorgonian species will remain unstable, despite larval behaviour is better
447 ascertained, making cross-validation with observed population genetics more hazardous
448 (Padrón et al., 2018b,a).

449 In conclusion, methodological choices are crucial when performing larval dispersal si-
450 mulations to guide biodiversity management. Specifically, advising the design of coastal
451 MPA with adequate regional connectivity estimates requires adapting flow simulation

452 resolution to the area. For species dwelling in rocky habitat such as gorgonians, flow
453 representation at a grid resolution sufficient to resolve the coastal dynamics in these en-
454 vironments is a bottleneck, and despite coastal dynamics may be very different from place
455 to place, the bathymetry steepness is likely to require horizontal resolution in the order
456 of a few hundred meters or less. In such a case, multiplying dispersal tracks to account
457 for turbulence effect can be avoided as the flow representation will already include most
458 of the subgrid variability, reducing computational costs. In contrast, estimating disper-
459 sal patterns variability arising from uncertainty on release timing by simulating multiple
460 release events and PLD range should be systematic to estimate confidence level for the
461 different connectivity patterns. These initial methodological choices do not preclude the
462 need to vary the larval vertical behaviour when known to span the range of variability
463 arising from species diversity.

464 **Supporting Information**

465 Supporting Information are available in online version of the manuscript.

466 **Acknowledgments**

467 This work was supported by the IMPACT EU funded project (PC Interreg VA IFM
468 2014-2020, Prot. ISMAR n. 0002269). The authors would also like to thank Francesco
469 Ferrari, Federico Cassola and Andrea Mazzino for providing the surface forcings for the
470 LIMEgcm setup used in this work and Anna Vetrano and Mireno Borghini for the ADCP
471 data collected in proximity of the MT Haven shipwreck. The data underlying this article
472 will be shared on reasonable request to the corresponding author.

473 **References**

474 Andrello, M., Mouillot, D., Beuvier, J., Albouy, C., Thuiller, W., and Manel, S. (2013).
475 Low connectivity between mediterranean marine protected areas: A biophysical model-

476 ing approach for the dusky grouper *epinephelus marginatus*. *PLOS ONE*, 8(7):1–15.

477 Barbut, L., Groot Crego, C., Delerue-Ricard, S., Vandamme, S., Volckaert, F. A. M.,
478 and Lacroix, G. (2019). How larval traits of six flatfish species impact connectivity.
479 *Limnology and Oceanography*, 64(3):1150–1171.

480 Beuvier, J., Béranger, K., Lebeau-pin Brossier, C., Somot, S., Sevault, F., Drillet, Y.,
481 Bourdallé-Badie, R., et al. (2012). Spreading of the western mediterranean deep water
482 after winter 2005: Time scales and deep cyclone transport. *Journal of Geophysical*
483 *Research: Oceans*, 117(C7).

484 Briton, F., Cortese, D., Duhaut, T., and Guizien, K. (2018). High-resolution modelling
485 of ocean circulation can reveal retention spots important for biodiversity conservation.
486 *Aquatic Conservation: Marine and Freshwater Ecosystems*, 28(4):882–893.

487 Carpine, C. and Grasshoff, M. (1975). Les gorgonaires de la méditerranée. *Bulletin de*
488 *l’Institut Océanographique de Monaco*, 71:1–140.

489 Cassola, F., Ferrari, F., and Mazzino, A. (2015). Numerical simulations of Mediterranean
490 heavy precipitation events with the WRF model: A verification exercise using different
491 approaches. *Atmospheric Research*, 164:210–225.

492 CBD (2010). Strategic plan for biodiversity 2011–2020. Secretariat of the Convention
493 on Biological Diversity Montreal, Canada.

494 Chia, F.-S., Buckland-Nicks, J., and Young, C. M. (1984). Locomotion of marine inver-
495 tebrate larvae: a review. *Canadian Journal of Zoology*, 62(7):1205–1222.

496 Coelho, M. A. and Lasker, H. R. (2014). Reproductive biology of the caribbean brooding
497 octocoral *antilloorgia hystrix*. *Invertebrate Biology*, 133(4):299–313.

498 Coelho, M. A. and Lasker, H. R. (2016). Larval behavior and settlement dynamics
499 of a ubiquitous caribbean octocoral and its implications for dispersal. *Marine Ecology*
500 *Progress Series*, 561:109–121.

501 Coma, R., Ribes, M., Zabala, M., and Gili, J.-M. (1995). Reproduction and cycle
502 of gonadal development in the mediterranean gorgonian paramuricea clavata. *Marine*
503 *Ecology Progress Series*, 117(1/3):173–183.

504 Corell, H., Moksnes, P.-O., Engqvist, A., Döös, K., and Jonsson, P. R. (2012). Depth dis-
505 tribution of larvae critically affects their dispersal and the efficiency of marine protected
506 areas. *Marine Ecology Progress Series*, 467:29–46.

507 Crosbie, T., Wright, D. W., Oppedal, F., Johnsen, I. A., Samsing, F., and Dempster, T.
508 (2019). Effects of step salinity gradients on salmon lice larvae behaviour and dispersal.
509 *Aquaculture Environment Interactions*, 11:181–190.

510 Dee, D. P., Uppala, S. M., Simmons, A. J., Berrisford, P., Poli, P., Kobayashi, S.,
511 Andrae, U., et al. (2011). The era-interim reanalysis: configuration and performance
512 of the data assimilation system. *Quarterly Journal of the Royal Meteorological Society*,
513 137(656):553–597.

514 Fine, M., Aluma, Y., Meroz-Fine, E., Abelson, A., and Loya, Y. (2005). *Acabaria*
515 *erythraea* (octocorallia: Gorgonacea) a successful invader to the mediterranean sea?
516 *Coral Reefs*, 24(1):161–164.

517 Gamoyo, M., Obura, D., and Reason, C. J. C. (2019). Estimating connectivity through
518 larval dispersal in the western indian ocean. *Journal of Geophysical Research: Biogeo-*
519 *sciences*, 124(8):2446–2459.

520 García-Monteiro, S., Sobrino, J., Julien, Y., Sória, G., and Skokovic, D. (2022). Surface
521 temperature trends in the mediterranean sea from modis data during years 2003-2019.
522 *Regional Studies in Marine Science*, 49:102086.

523 Gori, A., Bavestrello, G., Grinyó, J., Dominguez-Carrió, C., Ambroso, S., and Bo, M.
524 (2017). *Animal Forests in Deep Coastal Bottoms and Continental Shelf of the Mediter-*
525 *ranean Sea*, pages 1–27. Springer International Publishing, Cham.

526 Gori, A., Linares, C., Rossi, S., Coma, R., and Gili, J.-M. (2007). Spatial variability
527 in reproductive cycle of the gorgonians paramuricea clavata and eunicella singularis

528 (anthozoa, octocorallia) in the western mediterranean sea. *Marine Biology*, 151(4):1571–
529 1584.

530 Gori, A., Rossi, S., Berganzo, E., Pretus, J. L., Dale, M. R., and Gili, J.-M. (2011).
531 Spatial distribution patterns of the gorgonians eunicella singularis, paramuricea clavata,
532 and leptogorgia sarmentosa (cape of creus, northwestern mediterranean sea). *Marine*
533 *biology*, 158(1):143–158.

534 Graham, E., Baird, A., Connolly, S., Sewell, M., and Willis, B. (2013). Rapid declines
535 in metabolism explain extended coral larval longevity. *Coral Reefs*, 32(2):539–549.

536 Griffies, S. M. and Treguier, A. M. (2013). Chapter 20 - ocean circulation models
537 and modeling. In Siedler, G., Griffies, S. M., Gould, J., and Church, J. A., editors,
538 *Ocean Circulation and Climate*, volume 103 of *International Geophysics*, pages 521–551.
539 Academic Press.

540 Grüss, A., Kaplan, D. M., Guénette, S., Roberts, C. M., and Botsford, L. W. (2011).
541 Consequences of adult and juvenile movement for marine protected areas. *Biological*
542 *Conservation*, 144(2):692–702.

543 Guizien, K., Belharet, M., Marsaleix, P., and Guarini, J. M. (2012). Using larval dis-
544 persal simulations for marine protected area design: Application to the gulf of lions
545 (northwest mediterranean). *Limnology and Oceanography*, 57(4):1099–1112.

546 Guizien, K., Brochier, T., Duchene, J., Koh, B.-S., and Marsaleix, P. (2006). Dispersal
547 of owenia fusiformis larvae by wind-driven currents: turbulence, swimming behaviour
548 and mortality in a three-dimensional stochastic model. *Marine Ecology Progress Series*,
549 311:47–66.

550 Guizien, K., Viladrich, N., Martínez-Quintana, Á., and Bramanti, L. (2020). Survive
551 or swim: different relationships between migration potential and larval size in three
552 sympatric mediterranean octocorals. *Scientific reports*, 10(1):1–12.

553 Halpern, B. S. and Warner, R. R. (2003). Review paper. matching marine reserve design
554 to reserve objectives. *Proceedings of the Royal Society of London. Series B: Biological*
555 *Sciences*, 270(1527):1871–1878.

556 Hidalgo, M., Rossi, V., Monroy, P., Ser-Giacomi, E., Hernández-García, E., Guijarro, B.,
557 Massutí, E., Alemany, F., Jadaud, A., Perez, J. L., and Reglero, P. (2019). Accounting
558 for ocean connectivity and hydroclimate in fish recruitment fluctuations within trans-
559 boundary metapopulations. *Ecological Applications*, 29(5):e01913.

560 Hock, K., Doropoulos, C., Gorton, R., Condie, S. A., and Mumby, P. J. (2019). Split
561 spawning increases robustness of coral larval supply and inter-reef connectivity. *Nature*
562 *communications*, 10(1):1–10.

563 Huret, M., Runge, J. A., Chen, C., Cowles, G., Xu, Q., and Pringle, J. M. (2007).
564 Dispersal modeling of fish early life stages: sensitivity with application to atlantic cod
565 in the western gulf of maine. *Marine Ecology Progress Series*, 347:261–274.

566 Jackett, D. R. and McDougall, T. J. (1995). Minimal Adjustment of Hydrographic
567 Profiles to Achieve Static Stability. *Journal of Atmospheric and Oceanic Technology*,
568 12(2):381–389.

569 Jones, C. G., Lawton, J. H., and Shachak, M. (1994). Organisms as ecosystem engineers.
570 *Oikos*, 69(3):373–386.

571 Kenchington, E., Wang, Z., Lirette, C., Murillo, F. J., Guijarro, J., Yashayaev, I., and
572 Maldonado, M. (2019). Connectivity modelling of areas closed to protect vulnerable
573 marine ecosystems in the northwest atlantic. *Deep Sea Research Part I: Oceanographic*
574 *Research Papers*, 143:85–103.

575 Kough, A. S. and Paris, C. B. (2015). The influence of spawning periodicity on popu-
576 lation connectivity. *Coral Reefs*, 34(3):753–757.

577 Kvile, K. Ø., Romagnoni, G., Dagestad, K.-F., Langangen, Ø., and Kristiansen, T.
578 (2018). Sensitivity of modelled North Sea cod larvae transport to vertical behaviour,

579 ocean model resolution and interannual variation in ocean dynamics. *ICES Journal of*
580 *Marine Science*, 75(7):2413–2424.

581 Large, W. G., McWilliams, J. C., and Doney, S. C. (1994). Oceanic vertical mixing:
582 A review and a model with a nonlocal boundary layer parameterization. *Reviews of*
583 *Geophysics*, 32(4):363–403.

584 Leis, J. M. (2007). Behaviour as input for modelling dispersal of fish larvae: behaviour,
585 biogeography, hydrodynamics, ontogeny, physiology and phylogeny meet hydrography.
586 *Marine Ecology Progress Series*, 347:185–193.

587 Leis, J. M. (2021). Perspectives on larval behaviour in biophysical modelling of larval
588 dispersal in marine, demersal fishes. *Oceans*, 2(1):1–25.

589 Lett, C., Verley, P., Mullon, C., Parada, C., Brochier, T., Penven, P., and Blanke,
590 B. (2008). A lagrangian tool for modelling ichthyoplankton dynamics. *Environmental*
591 *Modelling & Software*, 23(9):1210–1214.

592 Linares, C., Coma, R., Mariani, S., Díaz, D., Hereu, B., and Zabala, M. (2008). Early life
593 history of the mediterranean gorgonian paramuricea clavata: implications for population
594 dynamics. *Invertebrate Biology*, 127(1):1–11.

595 Liu, G., Bracco, A., Quattrini, A. M., and Herrera, S. (2021). Kilometer-scale larval dis-
596 persal processes predict metapopulation connectivity pathways for paramuricea biscaya
597 in the northern gulf of mexico. *Frontiers in Marine Science*, 8.

598 Marshall, J., Adcroft, A., Hill, C., Perelman, L., and Heisey, C. (1997). A finite-volume,
599 incompressible Navier Stokes model for studies of the ocean on parallel computers. *J.*
600 *Geophys. Res.*, 102(C3):5753–5766.

601 Marta-Almeida, M., Dubert, J., Peliz, Á., and Queiroga, H. (2006). Influence of vertical
602 migration pattern on retention of crab larvae in a seasonal upwelling system. *Marine*
603 *Ecology Progress Series*, 307:1–19.

604 MedPAN, U. (2017). Map-spa/rac (2017). the 2016 status of marine protected ar-
605 eas in the mediterranean: Main findings. [https://drive.google.com/file/d/1-](https://drive.google.com/file/d/1-an1aHCqHP1xAJGHaRgKXqZ4-rTPbBzR/view)
606 [an1aHCqHP1xAJGHaRgKXqZ4-rTPbBzR/view](https://drive.google.com/file/d/1-an1aHCqHP1xAJGHaRgKXqZ4-rTPbBzR/view).

607 Metaxas, A., Lacharité, M., and de Mendonça, S. N. (2019). Hydrodynamic connectivity
608 of habitats of deep-water corals in corsair canyon, northwest atlantic: A case for cross-
609 boundary conservation. *Frontiers in Marine Science*, 6.

610 Millot, C. (1999). Circulation in the western mediterranean sea. *Journal of Marine*
611 *Systems*, 20(1):423–442.

612 Mokhtar-Jamaï, K., Pascual, M., Ledoux, J.-B., Coma, R., Féral, J.-P., Garrabou, J.,
613 and Aurelle, D. (2011). From global to local genetic structuring in the red gorgonian
614 *paramuricea clavata*: the interplay between oceanographic conditions and limited larval
615 dispersal. *Molecular Ecology*, 20(16):3291–3305.

616 Munk, W. H. (1966). Abyssal recipes. *Deep Sea Research and Oceanographic Abstracts*,
617 13(4):707–730.

618 North, E. W., Gallego, A., and Petitgas, P. (2009). Manual of recommended practices
619 for modelling physical–biological interactions during fish early life. *ICES Cooperative*
620 *Research Report*, 295:112.

621 North, E. W., Schlag, Z., Hood, R. R., Li, M., Zhong, L., Gross, T., and Kennedy, V. S.
622 (2008). Vertical swimming behavior influences the dispersal of simulated oyster larvae in
623 a coupled particle-tracking and hydrodynamic model of chesapeake bay. *Marine Ecology*
624 *Progress Series*, 359:99–115.

625 Ospina-Alvarez, A., Weidberg, N., Aiken, C. M., and Navarrete, S. A. (2018). Larval
626 transport in the upwelling ecosystem of central chile: The effects of vertical migration,
627 developmental time and coastal topography on recruitment. *Progress in Oceanography*,
628 168:82–99.

629 Padrón, M., Costantini, F., Baksay, S., Bramanti, L., and Guizien, K. (2018a). Passive
630 larval transport explains recent gene flow in a mediterranean gorgonian. *Coral Reefs*,
631 37:495–506.

632 Padrón, M., Costantini, F., Bramanti, L., Guizien, K., and Abbiati, M. (2018b). Genetic
633 connectivity supports recovery of gorgonian populations affected by climate change.
634 *Aquatic Conservation: Marine and Freshwater Ecosystems*, 28(4):776–787.

635 Paris, C. B., Helgers, J., van Sebille, E., and Srinivasan, A. (2013). Connectivity mod-
636 eling system: A probabilistic modeling tool for the multi-scale tracking of biotic and
637 abiotic variability in the ocean. *Environmental Modelling & Software*, 42:47–54.

638 Pineda, J., Hare, J. A., and Sponaugle, S. (2007). Larval transport and dispersal in the
639 coastal ocean and consequences for population connectivity. *Oceanography*, 20.

640 Ponti, M., Grech, D., Mori, M., Perlini, R., Ventra, V., Panzalis, P., and Cerrano, C.
641 (2016). The role of gorgonians on the diversity of vagile benthic fauna in mediterranean
642 rocky habitats. *Marine Biology*, 163.

643 Putman, N. F. and He, R. (2013). Tracking the long-distance dispersal of marine or-
644 ganisms: sensitivity to ocean model resolution. *Journal of the Royal Society Interface*,
645 10(81):20120979.

646 Queiroga, H., Cruz, T., dos Santos, A., Dubert, J., González-Gordillo, J. I., Paula, J.,
647 Álvaro Peliz, and Santos, A. M. P. (2007). Oceanographic and behavioural processes
648 affecting invertebrate larval dispersal and supply in the western iberia upwelling ecosys-
649 tem. *Progress in Oceanography*, 74(2):174–191.

650 Ribes, M., Coma, R., Rossi, S., and Micheli, M. (2007). Cycle of gonadal development in
651 *eunicella singularis* (cnidaria: Octocorallia): trends in sexual reproduction in gorgonians.
652 *Invertebrate Biology*, 126(4):307–317.

653 Rossi, V., Lo, M., Legrand, T., Ser-Giacomi, E., de Jode, A., Thierry De Ville D'avray,
654 L., Pairaud, I., Faure, V., Fraysse, M., Pinazo, C., and Chenuil, A. (2020). Small-

655 scale connectivity of coralligenous habitats: insights from a modelling approach within
656 a semi-opened mediterranean bay.

657 Rossi, V., Ser-Giacomi, E., López, C., and Hernández-García, E. (2014). Hydrodynamic
658 provinces and oceanic connectivity from a transport network help designing marine
659 reserves. *Geophysical Research Letters*, 41(8):2883–2891.

660 Rumrill, S. S. (1990). Natural mortality of marine invertebrate larvae. *Ophelia*, 32(1-
661 2):163–198.

662 Scheltema, R. S. (1986). On dispersal and planktonic larvae of benthic invertebrates: An
663 eclectic overview and summary of problems. *Bulletin of Marine Science*, 39(2):290–322.

664 Schlag, Z. R. and North, E. W. (2012). *Lagrangian TRANSport model (LTRANS v.2)*
665 *User’s Guide*. University of Maryland Center for Environmental Science, Horn Point
666 Laboratory.

667 Schroeder, K., Chiggiato, J., Bryden, H., Borghini, M., and Ismail, S. B. (2016). Abrupt
668 climate shift in the western mediterranean sea. *Scientific Reports*, 6.

669 Sciascia, R., Magaldi, M. G., and Vetrano, A. (2019). Current reversal and associated
670 variability within the corsica channel: The 2004 case study. *Deep Sea Research Part I:*
671 *Oceanographic Research Papers*, 144:39 – 51.

672 Shchepetkin, A. F. and McWilliams, J. C. (2005). The regional oceanic modeling system
673 (ROMS): a split-explicit, free-surface, topography-following-coordinate oceanic model.
674 *Ocean Modelling*, 9(4):347 – 404.

675 Simons, R. D., Siegel, D. A., and Brown, K. S. (2013). Model sensitivity and robustness
676 in the estimation of larval transport: A study of particle tracking parameters. *Journal*
677 *of Marine Systems*, 119-120:19–29.

678 Swearer, S. E., Treml, E. A., and Shima, J. S. (2019). *A Review of Biophysical Models*
679 *of Marine Larval Dispersal*. Taylor & Francis.

680 Tremblay, M. J., Loder, J. W., Werner, F. E., Naimie, C. E., Page, F. H., and Sinclair,
681 M. M. (1994). Drift of sea scallop larvae *Placopecten magellanicus* on Georges Bank: a
682 model study of the roles of mean advection, larval behavior and larval origin. *Deep Sea*
683 *Research Part II: Topical Studies in Oceanography*, 41(1):7 – 49.

684 Urban, M. C., Bocedi, G., Hendry, A. P., Mihoub, J.-B., Pe'er, G., Singer, A., Bridle,
685 J. R., Crozier, L. G., De Meester, L., Godsoe, W., Gonzalez, A., Hellmann, J. J., Holt,
686 R. D., Huth, A., Johst, K., Krug, C. B., Leadley, P. W., Palmer, S. C. F., Pantel, J. H.,
687 Schmitz, A., Zollner, P. A., and Travis, J. M. J. (2016). Improving the forecast for
688 biodiversity under climate change. *Science*, 353(6304).

689 Vignudelli, S., Gasparini, G., Astraldi, M., and Schiano, M. (1999). A possible influence
690 of the North Atlantic Oscillation on the circulation of the Western Mediterranean Sea.
691 *Geophysical Research Letters*, 26(5):623–626.

692 Wood, S., Paris, C. B., Ridgwell, A., and Hendy, E. J. (2014). Modelling dispersal
693 and connectivity of broadcast spawning corals at the global scale. *Global Ecology and*
694 *Biogeography*, 23(1):1–11.

695 Zelli, E., Quéré, G., Lago, N., Di Franco, G., Costantini, F., Rossi, S., and Bramanti,
696 L. (2020). Settlement dynamics and recruitment responses of Mediterranean gorgonian
697 larvae to different crustose coralline algae species. *Journal of Experimental Marine*
698 *Biology and Ecology*, 530-531:151427.

699 **Supporting Information**

Location (name code)	Longitude [deg. E]	Latitude [deg. N]	Coarse Resolution Depth [m]	Fine Resolution Depth [m]
Bergeggi (BER)	8.4550	44.2399	-28	-88
	8.4550	44.2349	-32	-102
	8.4550	44.2449	-24	-52
	8.4550	44.2299	-36	-133
	8.4550	44.2499	-22	-25
	8.4450	44.2249	-25	-133
	8.4600	44.2399	-36	-110
	8.4500	44.2249	-32	-150
	8.4600	44.2449	-31	-90
Portofino (POR)	9.2200	44.2899	-27	-52
	9.2150	44.2899	-24	-38
	9.2250	44.2899	-34	-63
	9.2100	44.2899	-22	-26
	9.2349	44.299	-31	-63
	9.2200	44.2849	-36	-75
	9.2349	44.3049	-24	-52
	9.2349	44.2949	-38	-63
	9.2150	44.2849	-32	-63
Sestri Levante (SES)	9.2100	44.2849	-30	-50
	9.3950	44.2449	-34	-9
	9.3900	44.2499	-33	-12
	9.4000	44.2449	-29	-12
	9.3900	44.2549	-26	-3
	9.4000	44.2399	-38	-33
	9.4050	44.2449	-23	-3
	9.3850	44.2549	-32	-12
	9.3850	44.2599	-24	-7
Punta Mesco (PTM)	9.4050	44.2399	-31	-26
	9.3800	44.2549	-38	-25
	9.6300	44.1199	-20	-33
	9.2500	44.1199	-22	-30
	9.6300	44.1149	-28	-42
	9.6200	44.1199	-28	-33
	9.6250	44.1149	-30	-52
	9.6350	44.1149	-26	-42
	9.6200	44.1149	-38	-52
Porto Venere (PRV)	9.6400	44.1149	-24	-25
	9.6300	44.1099	-35	-52
	9.6150	44.1199	-35	-42
	9.8350	44.0149	-21	-12
	9.8400	44.0099	-21	-18
	9.8500	44.0049	-22	-18
	9.8550	44.0049	-21	-18
	9.8450	44.0049	22	-18
	9.8350	44.0099	-24	-18
Porto Venere (PRV)	9.8599	44.0049	-20	-18
	9.8400	44.0049	-24	-18
	9.8300	44.0149	-23	-12
	9.8350	44.0049	-26	-18

Table S1: Longitudes, latitudes and depths of the release points for each population in the Ligurian Sea. Longitudes and latitudes are the same for both models while depths vary between the fine and coarse resolution model.

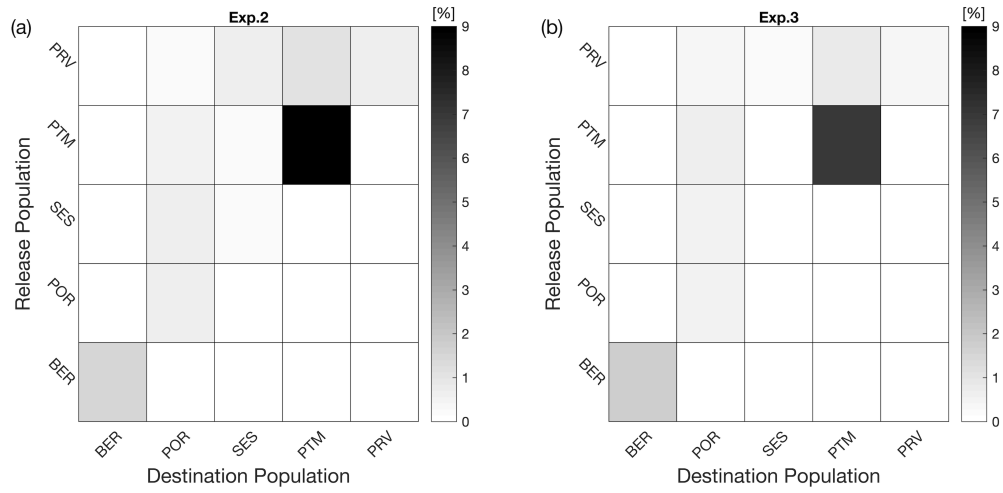


Figure S1: Median connectivity matrix for a PLD of 3.5 days and a 3-day release duration in (a) Exp.2 with fine resolution flow representation updated every 6h and in (b) Exp.3 with fine resolution flow representation updated every 3h.

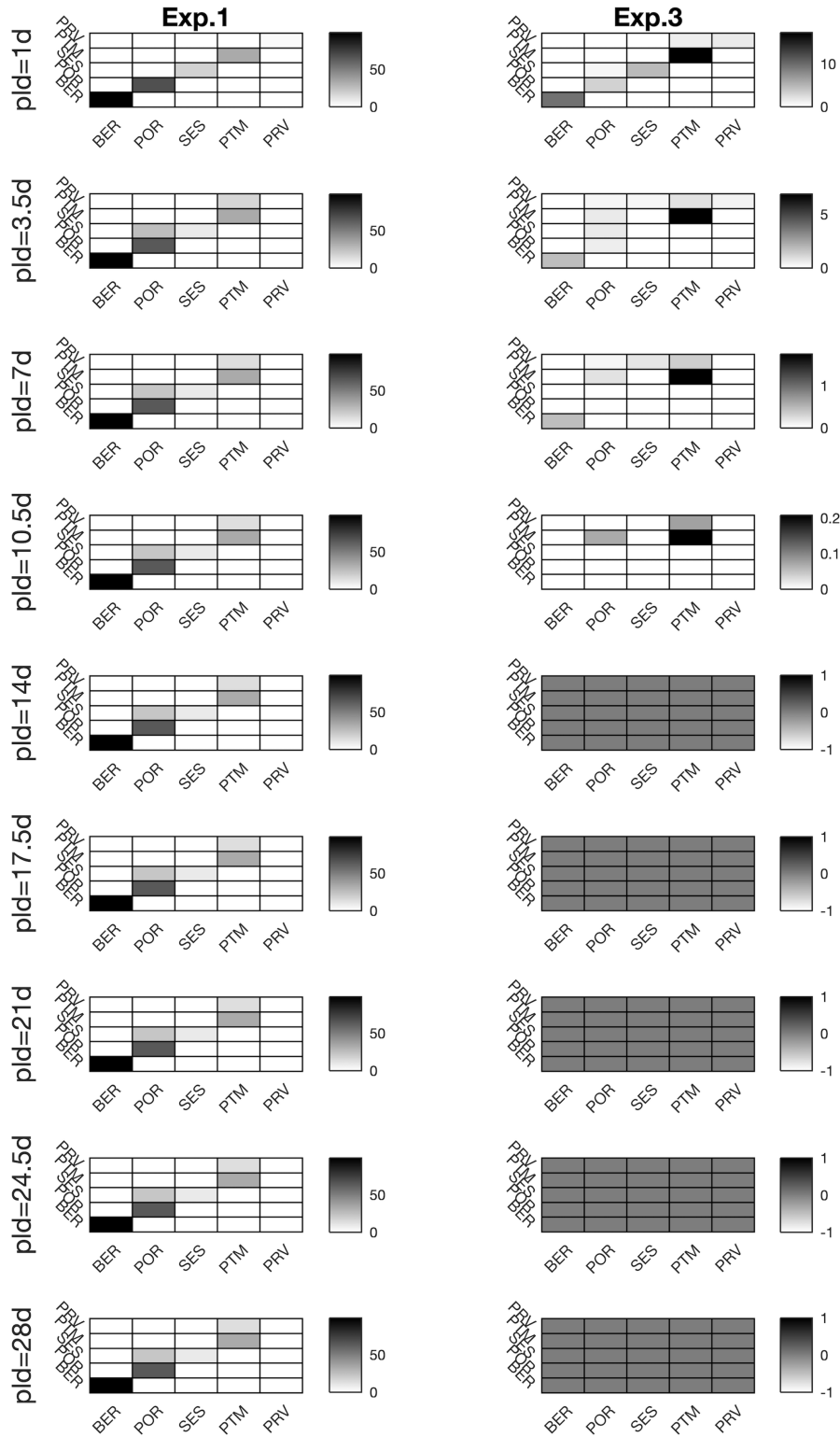


Figure S2: Median connectivity matrix for all PLDs and a 3-day release duration. The panels on the left display Exp.1 with coarse resolution flow representation updated every 6h and the panels on the right display Exp.3 with the fine resolution flow representation updated every 3h.

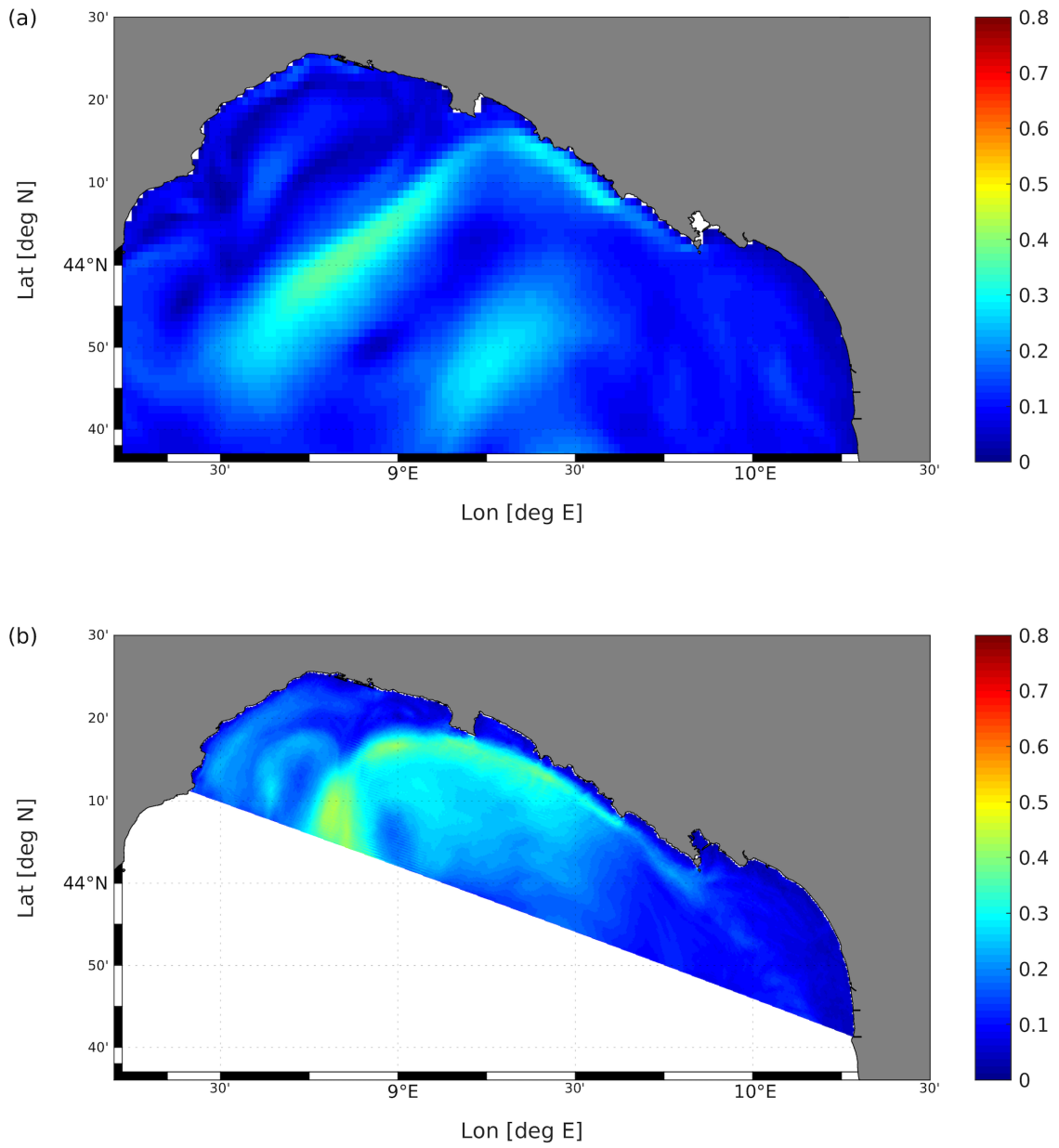


Figure S3: Surface speed on June 30th 2004 simulated at (a) coarse and (b) fine resolution.

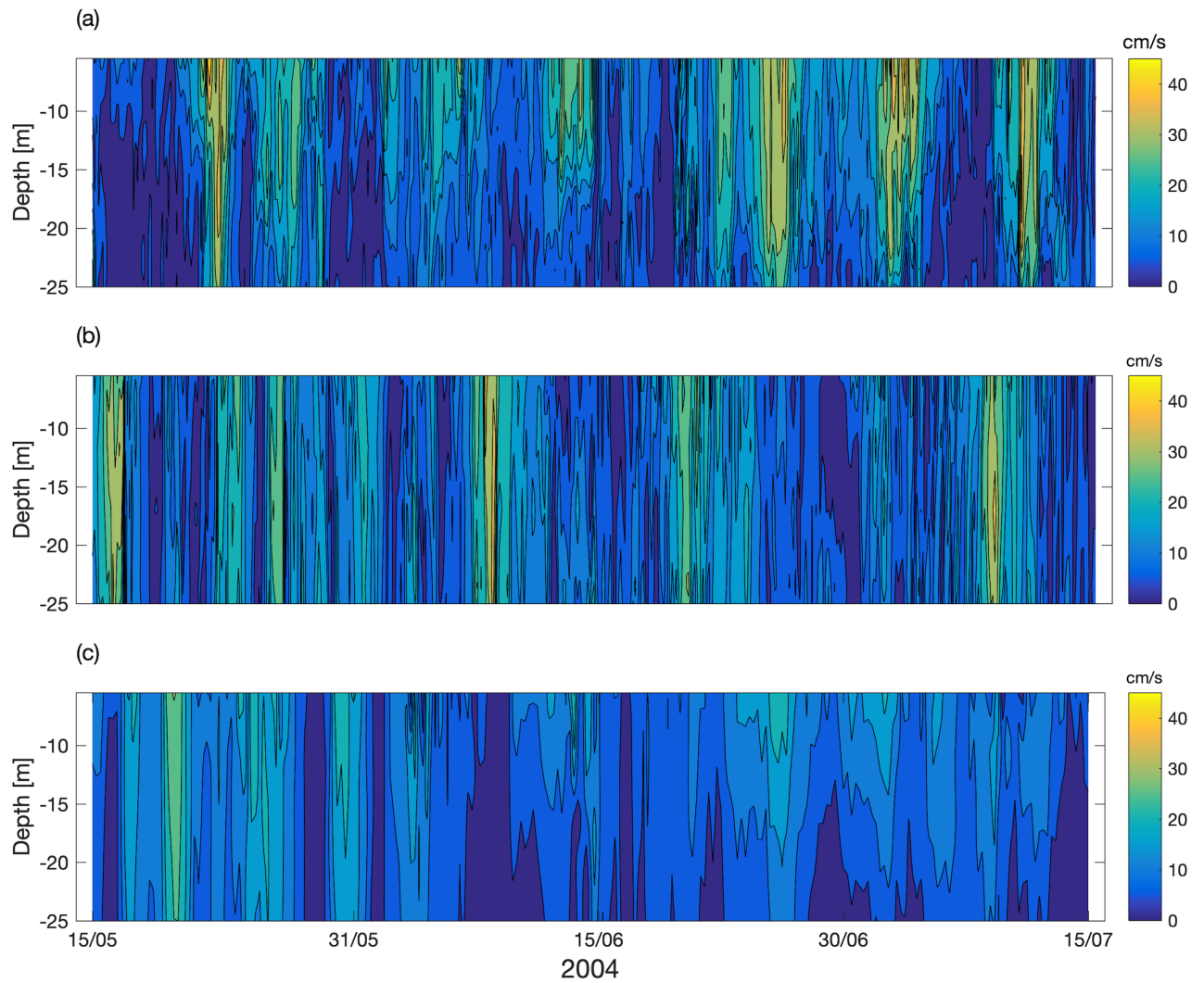


Figure S4: Current as a function of depth and time (15/05/2004-15/07/2004) in (a) observations, (b) the fine resolution 3D flow simulation, (c) the coarse resolution 3D flow simulation. Observations were taken from an Acoustic Doppler Current Profiler (ADCP) located in the vicinity of the MT Haven shipwreck in the Ligurian Sea (44.37N, 8.70E). Flow simulation data are obtained from the closest grid points to the ADCP location.

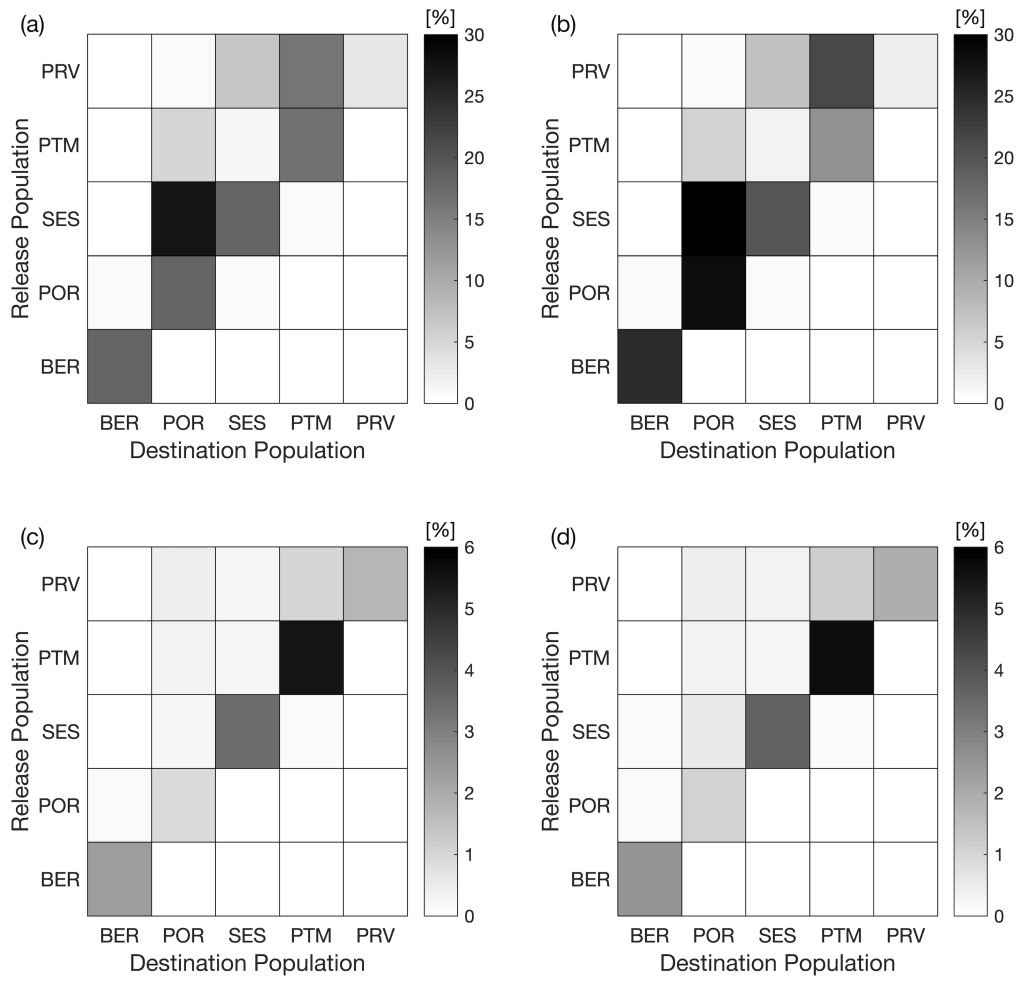


Figure S5: Connectivity matrix for the larval release events of 2004 and 2006 for the *E. singularis* behaviour simulations without turbulence and a PLD of 3.5 days. Panels (a) and (b) represent the σ_{intra} and σ_{inter} for Exp.1, panels (c) and (d) represent the σ_{intra} and σ_{inter} for Exp.3.